

Butyl Pocket Formation in the Vitamin D Receptor Strongly Affects the Agonistic or Antagonistic Behavior of Ligands

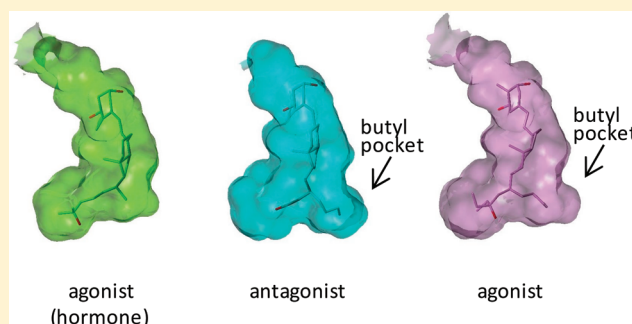
Nobuko Yoshimoto,^{†,‡,⊥} Yuta Sakamaki,^{†,§,⊥} Minoru Haeta,[†] Akira Kato,[†] Yuka Inaba,[†] Toshimasa Itoh,[†] Makoto Nakabayashi,^{||} Nobutoshi Ito,^{||} and Keiko Yamamoto^{*,†,‡}

[†]Laboratory of Drug Design and Medicinal Chemistry and [‡]High Technology Research Center, Showa Pharmaceutical University, 3-3165 Higashi-Tamagawagakuen, Machida, Tokyo 194-8543, Japan

[§]Institute of Biomaterials and Bioengineering, Tokyo Medical and Dental University, 2-3-10 Kanda-Surugadai, Chiyoda-ku, Tokyo 101-0062, Japan

^{||}Graduate School of Biomedical Science, Tokyo Medical and Dental University, Bunkyo-ku, Tokyo 113-8510, Japan

ABSTRACT: Previously, we reported that 22*S*-butyl-25,26,27-trinor-1 α ,24-dihydroxyvitamin D₃ **2** represents a new class of antagonist for the vitamin D receptor (VDR). The crystal structure of the ligand-binding domain (LBD) of VDR complexed with **2** showed the formation of a butyl pocket to accommodate the 22-butyl group and insufficient interactions between ligand **2** and the C-terminus of VDR. Here, we designed and synthesized new analogues **5a–c** and evaluated their biological activities to probe whether agonistic activity is recovered when the analogue restores interactions with the C-terminus of VDR. Analogues **5a–c** exhibited full agonistic activity in transactivation. Interestingly, **5c**, which bears a 24-diethyl group, completely recovered agonistic activity, although **3c** and **4c** act as an antagonist and a weak agonist, respectively. The crystal structures of VDR-LBD complexed with **3a**, **4a**, **5a**, and **5c** were solved, and the results confirmed that butyl pocket formation in VDR strongly affects the agonistic or antagonistic behaviors of ligands.



■ INTRODUCTION

Active vitamin D₃, 1 α ,25-dihydroxyvitamin D₃ **1a** (Chart 1), is a hormone that plays a major role in calcium homeostasis. This hormone is also involved in cell differentiation and proliferation and immunomodulation.¹ The actions of **1a** and its active analogues are mediated by the vitamin D receptor (VDR), which is a member of the nuclear receptor superfamily that includes the receptors for steroid, retinoid, and thyroid hormones.² These nuclear receptors function through a common mechanism by which the receptors regulate the transcription of their target genes. VDR forms a heterodimer with retinoid X receptor (RXR), and upon ligand binding, VDR changes to an active conformation that provides the activation function 2 (AF2) surface to allow binding of a coactivator.³

Since the discovery of **1a**, thousands of vitamin D analogues have been synthesized,³ of which more than 10 have been clinically used to treat metabolic bone diseases and skin diseases such as psoriasis, immune disorders, and malignant tumors.^{4,5} All these clinically used analogues are VDR agonists. VDR antagonists have been synthesized by several groups and are classified structurally into two types. The first group is composed of analogues containing a bulky side chain, such as carboxylic ester (ZK series) compounds⁶ and adamantane compounds,⁷ while the second group is composed of analogues lacking a bulky side chain, such as (23*S*)-25-dehydro-1 α -hydroxyvitamin D₃-26,23-lactone (TEI9647)⁸ and its deriva-

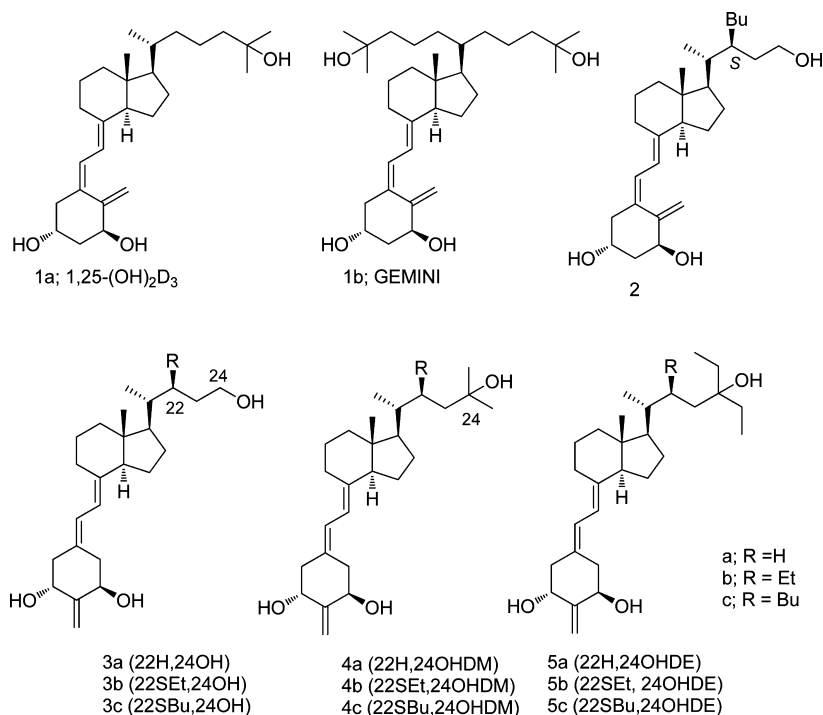
tives.^{8–11} VDR antagonism is believed to be based on an unstable conformation of VDR generated upon ligand binding. A VDR that accommodates an antagonist would prevent the heterodimerization with RXR and/or the recruitment of coactivators. However, the molecular basis for VDR antagonism is not clearly understood.

Recently, we reported that 22*S*-butyl-25,26,27-trinor-1 α ,24-dihydroxyvitamin D₃ **2** acts as a third type of VDR antagonist.¹² The crystal structure of the ligand binding domain (LBD) of VDR complexed with **2** shows the formation of an extra cavity to accommodate the butyl group.¹² We have termed this extra cavity the “butyl pocket”. Several research groups have solved crystal structures of VDR-LBD complexed with a variety of ligands.^{13–25} Most of the crystal structures show the canonical Moras’ active conformation¹³ of VDR-LBD and similar architectures of the ligand binding pocket (LBP). Exceptions are the complex of zebrafish VDR-LBD with “GEMINI”,^{16,20} which has two identical side chains,^{26,27} and the complex of VDR-LBD with 22-butyl analogue **2**.¹² The crystal structure of the zebrafish VDR-LBD/GEMINI complex revealed the formation of a new cavity, which is an extension of the original LBP, in order to accommodate the second side chain. The crystal structure of the VDR-LBD/**2** complex also revealed the

Received: February 21, 2012

Published: April 18, 2012

Chart 1. Structures of 1a and Vitamin D Analogues



formation of a cavity similar to that of the VDR-LBD/GEMINI complex. These observations suggest that the region around helix 6, loop 6–7, and the N-terminus of helix 7 is somewhat flexible. Interestingly, although both GEMINI **1b** and 22-butyl analogue **2** induce the formation of an extra cavity, **1b** acts as a VDR agonist whereas **2** acts as a VDR antagonist. We hypothesized that the contrasting behaviors of **1b** and **2** against VDR were derived from differences in hydrophobic interactions between the side chain terminus of each ligand and the C-terminus of VDR.

To investigate the effects on antagonism of the induction of the butyl pocket and of insufficient interactions of the ligand with the C-terminus of VDR, we synthesized a series of vitamin D₃ analogues with and without a 22-alkyl substituent and evaluated their biological activities.²⁸ We found that these synthetic ligands show strong antagonist, partial agonist, or full agonist activities, depending on the primary or tertiary alcohol at the side chain terminus and on the length of the 22-alkyl group. The results suggested that both the induction of a butyl pocket and insufficient hydrophobic interactions with the VDR C-terminus are necessary for VDR antagonism.

The present study was conducted to further confirm the molecular basis of agonistic and antagonistic activity of a new class of ligands that induce the formation of a butyl pocket. Here, we report the design, synthesis, and biological evaluation of new analogues in order to probe whether agonistic activity increases when the analogue exhibits increased interactions with the C-terminus of VDR. Furthermore, X-ray crystallographic analyses of VDR-LBD complexed with those analogues, which contain or lack a 22-butyl substituent, are also reported.

DESIGN AND SYNTHESIS

Design. Previously we showed that a 22-butyl analogue with a 24-primary alcohol, **3c**, is a VDR ligand but does not activate VDR whereas the corresponding 24-tertiary alcohol **4c** activates VDR, albeit weakly.²⁸ The results implied that the introduction

of a more hydrophobic substituent at the 24-position would enhance VDR activation. Therefore, we designed 22-butyl analogue **5c** with a diethyl substituent instead of a dimethyl at C(24). 22-Ethyl analogue **5b** and 22-H analogue **5a**, both of which have a diethyl substituent at C(24), were also designed as counterparts of **5c**. As described in earlier paper, we selected the 2-methylene-19-nor structure because of its superior chemical stability, convenient synthesis, and its increased biological activity compared to the original A-ring structure.^{28,29}

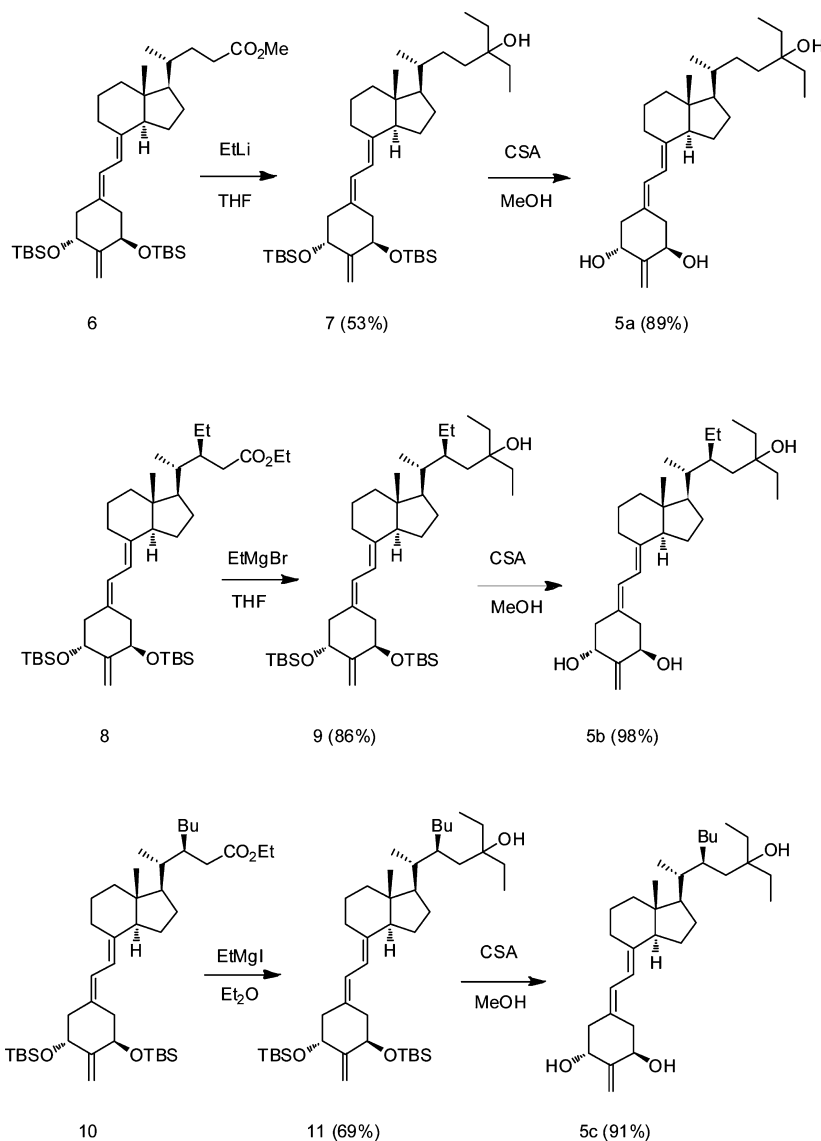
Synthesis of the 1,24-Dihydroxyvitamin D₃ Analogues. As shown in Scheme 1, 1,24-dihydroxyvitamin D₃ derivative **5a** was synthesized from ester **6**. Ester **6**, prepared by the procedure reported previously,²⁸ was treated with ethyllithium in THF to afford 24,24-diethylated compound **7**. Diethyl compound **7** was deprotected with CSA in methanol to provide desired compound **5a**. 22-Ethyl analogue **5b** was derived from 22-ethyl ester **8**.^{28,30} Ester **8** was treated with EtMgBr to afford 24,24-diethylated compound **9**. Compound **9** was deprotected with CSA in methanol to provide desired compound **5b**. 22-Butyl analogue **5c** was derived from 22-butyl ester **10**.^{28,30} Ester **10** was treated with EtMgI to afford 24,24-diethylated compound **11**. Compound **11** was deprotected with CSA in methanol to provide desired compound **5c**.

BIOLOGICAL ACTIVITIES

VDR Binding. Binding affinity to VDR was evaluated by a competitive binding assay using recombinant human VDR-LBD expressed as a C-terminus GST-tagged protein using the pGEX-VDR vector^{28,31} in *Escherichia coli* BL21. The results are summarized in Table 1 including previously reported results.²⁸ Three synthetic compounds **5a–c** showed specific binding to VDR, indicating they are ligands for VDR. In particular, **5a** showed stronger affinity than **1a**.

Transactivation. The ability of synthetic compounds **5a–c** to induce transcription of a vitamin D-responsive gene was tested using the mouse osteopontin luciferase reporter gene

Scheme 1. Synthesis of Compounds 5a–c



assay system in Cos7 cells.¹² The results are shown in Figure 1, together with the results for 3a–c and 4a–c.²⁸ New analogues 5a–c showed concentration-dependent transcriptional activity and acted as potent agonists. Of the 22-butyl analogues, new

Table 1. VDR Binding Affinity of Synthetic Analogues 3–6, IC₅₀ (nM)^a

Compd.	1a	3	4	5
a: R = H	0.08	2.7	0.10	0.029
b: R = Et		0.88	0.72	0.38
c: R = Bu		0.13	0.21	0.41

^aCompetitive binding of 1a and synthetic compounds 5a–c to the human vitamin D receptor. Affinity of related compounds (3a–c and 4a–c) was cited from previous report²⁸ to compare with 5a–c. The experiments were carried out in duplicate. The IC₅₀ values are derived from dose–response curves and represent the compound concentration required for 50% displacement of radiolabeled 1 α ,25-dihydroxyvitamin D₃ from the receptor protein.

analogue 5c completely restored full agonistic activity. In the 22-H analogues, the EC₅₀ of transcriptional activity decreased in the order 24OH 3a > 24OHDM 4a > 24OHDE 5a. In the 22-Et analogues, it is interesting that 5b acted as a full agonist while 3b and 4b are partial agonists.

■ X-RAY CRYSTAL STRUCTURE

We attempted to crystallize the VDR-LBD complex with the 22-H analogues (3a, 4a, and 5a) and 22-butyl analogues (3c, 4c, and 5c). We were able to obtain crystals in the presence of, but not in the absence of, a coactivator peptide, which is the same result as in our previous report.¹² Good quality crystals of VDR complexed with 3a, 4a, 5a, or 5c were obtained, but good crystals accommodating antagonists 3c or 4c were not obtained. As a result, we could solve the crystal structure of the complex with 3a, 4a, 5a (Figure 2), or 5c (Figure 3) but not the complex with 3c or 4c. The crystallographic analysis data are summarized in Table 2. The overall protein structure of VDR-LBD complexed with 3a, 4a, 5a, or 5c adopted the canonical Moras' active conformation observed in the complex with 1a.¹³ Coactivator peptide is also closely bound to the AF2

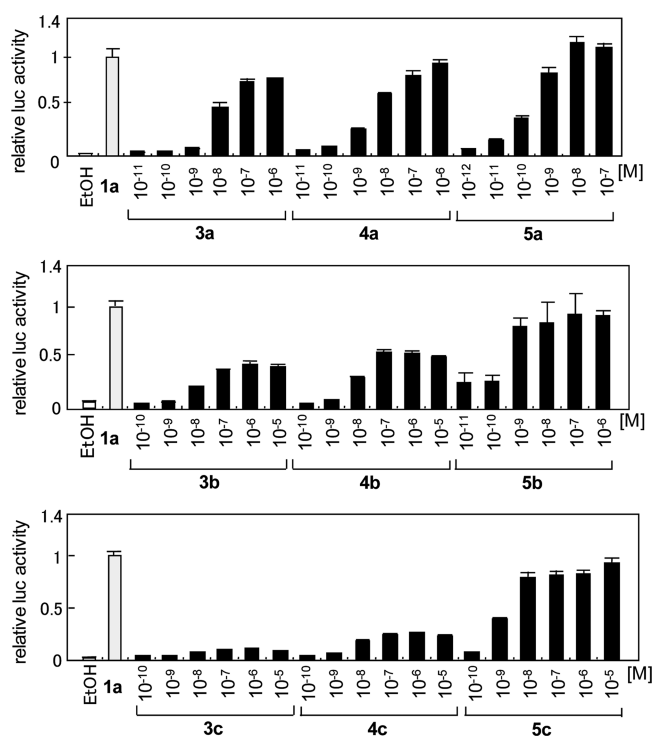


Figure 1. Transactivation of compounds 5a–c in Cos7 cells, together with the results of 3a–c and 4a–c previously reported.²⁸ Transcriptional activity was evaluated by the dual luciferase assay using a full-length human VDR expression plasmid (pCMX-hVDR), a reporter plasmid containing three copies of mouse osteopontin VDRE (SPPx3-TK-Luc), and an internal control plasmid containing sea pansy luciferase expression constructs (pRL-CMV) in Cos7 cells as described previously.¹² Luciferase activity of 10^{-8} M **1a** was defined as 1.

surface. These results indicate that the complexes with **3c** or **4c**, for which good quality crystals were not obtained, are difficult to adopt the canonical Moras' active conformation.

The entire main-chain structure of the VDR-LBD/5c complex is similar to the complex with **1a** or antagonist **2**. The 1α -, 3β -, and 25-hydroxyl groups of **5c** form pincer-type hydrogen bonds, as is the case with most vitamin D analogues (Figure 3a). Formation of a butyl pocket to accommodate the 22-butyl group was clearly observed (Figure 3b). The residues within 4.5 Å from each ligand are summarized in Table 3; these residues in **5c** are identical with those, except Leu400, in **1a**.

In the complexes with **3a**, **4a**, or **5a**, the side chain conformations of the amino acid residues lining the LBP are superimposed onto those of the VDR-LBD/**1a** complex. In the crystallographic analysis, ligands **4a** and **5a** docked in the VDR are well-defined, whereas the electron density map of the side chain of ligand **3a** in the VDR is unclear, probably because of its flexibility. Therefore, the side chain conformation of **3a** was tentatively determined based on the electron density map and the conformation that allowed hydrogen bonding with His393 and/or His301. Ligands **3a**, **4a**, and **5a** were accommodated into the VDR-LBP in a manner similar to **1a**. The hydroxyl groups at the 1α and 3β positions form pincer-type hydrogen bonds, evident in the VDR-LBD/**1a** complex (Figure 2a). Furthermore, the 24-hydroxyl group of **4a** and **5a** forms hydrogen bonds with both His393 and His301, and that of **3a** forms a hydrogen bond with His393 (Figure 2a). As shown in Table 3, compared with the complex with **1a**, complexes with **3a** and **4a** showed reduced interactions.

DISCUSSION

All synthetic analogues with a 24-hydroxyl group at the side chain showed specific binding to hVDR (Table 1). Therefore, compounds **5a–c** synthesized here are true ligands for hVDR. Interestingly, compound **5a** showed stronger affinity for hVDR

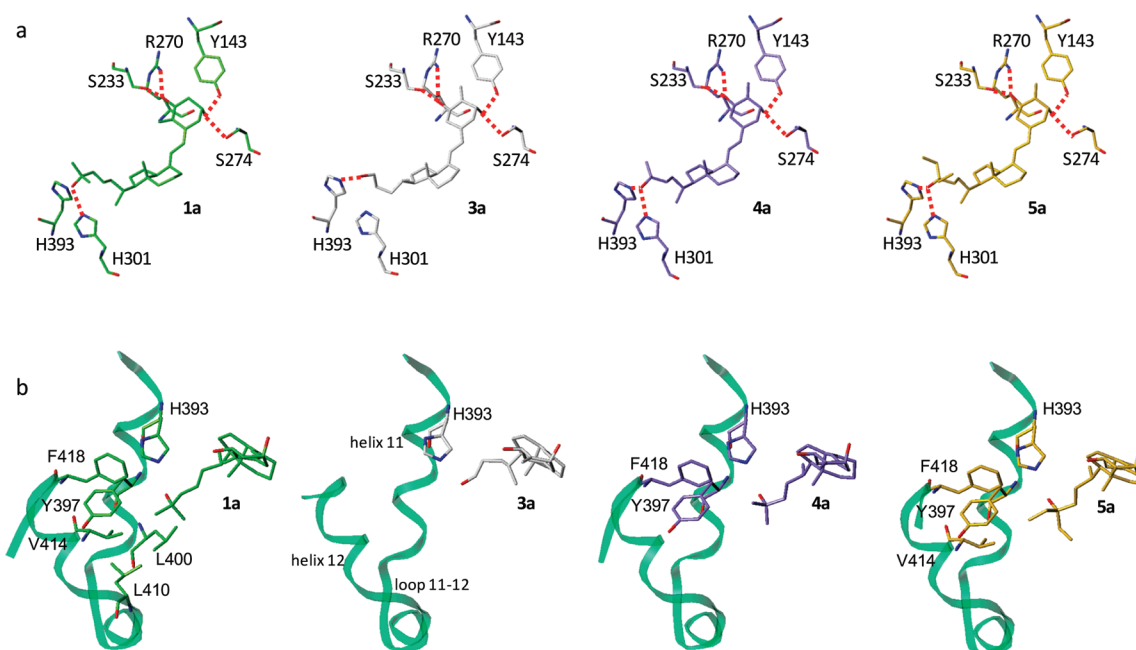


Figure 2. Crystal structures of VDR-LBD complexed with **1a**, **3a**, **4a**, and **5a**: (a) hydrogen bonds between VDR-LBD and **1a** (green), **3a** (gray), **4a** (purple), or **5a** (yellow); (b) interactions between the VDR C-terminus (helix 11, loop 11–12, and helix 12) and the ligands. The C-terminus (helix 11, loop 11–12, and helix 12) is presented as a green ribbon, and the ligands are presented in the same colors as in (a). Residues within 4.5 Å from each ligand are presented.

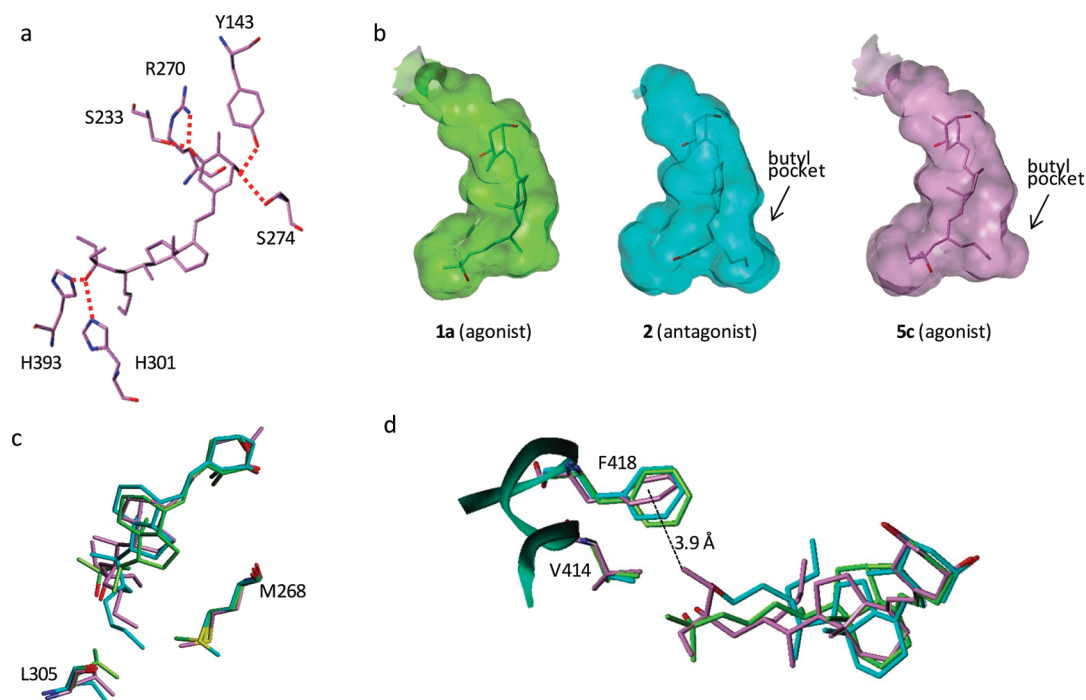


Figure 3. Crystal structures of VDR-LBD complexed with **5c**: (a) hydrogen bonds between VDR-LBD and **5c** (pink); (b) Connolly channel surface of the ligand-binding pocket of the VDR-LBD/**1a** complex (left, green), VDR-LBD/**2** complex (middle, cyan), and VDR-LBD/**5c** complex (right, pink); (c, d) superposition of VDR-LBD complexed with **1a** (green), **2** (cyan), or **5c** (pink). (a) The 1α -, 3β -, and 25 -hydroxyl groups of **5c** form pincer-type hydrogen bonds with Ser233 and Arg270, Tyr143 and Ser274, and His301 and His393, respectively. (b) Formation of the butyl pocket to accommodate the 22-butyl group is clearly observed in the complex with **2** and **5c**. (c) The terminal *S*-methyl group of Met268 in the VDR/**2** complex (cyan) rotated in about 120° compared with that in VDR/**1a** complex (green), but that in VDR/**5c** (pink) did not rotate. Leu305 in VDR/**5c** (pink) adopted intermediate conformation between conformations of the complexes with **1a** and **2**. (d) **5c** (pink) and Phe418 at helix 12 make C–H $\cdots\pi$ interactions. The distance between the terminal carbon of one of 24-ethyl groups in **5c** and the center of the π -system ($d_{C-\pi}$) is 3.9 Å.

Table 2. Summary of Data Collection Statistics and Refinement

parameter	ligand			
	3a	4a	5a	5c
X-ray source	KEK-PF BL-6A	KEK-PFAR NW-12A	KEK-PFAR NW-12A	KEK-PFAR NW-12A
wavelength (Å)	0.97800	1.00000	1.00000	1.00000
space group	C2	C2	C2	C2
unit cell dimensions				
bond (Å)	$a = 152.99, b = 43.87, c = 42.43$	$a = 154.34, b = 42.29, c = 42.21$	$a = 154.14, b = 42.77, c = 42.12$	$a = 154.21, b = 43.21, c = 42.38$
angle (deg)	$\alpha = 90.00, \beta = 95.94, \gamma = 90.00$	$\alpha = 90.00, \beta = 95.89, \gamma = 90.00$	$\alpha = 90.00, \beta = 95.42, \gamma = 90.00$	$\alpha = 90.00, \beta = 95.49, \gamma = 90.00$
resolution range (Å) ^a	38.04–2.40 (2.49–2.40)	76.76–2.00 (2.11–2.00)	76.73–1.90 (2.00–1.90)	76.75–2.40 (2.53–2.40)
total no. of reflections	41156	56092	75735	34783
no. of unique reflections	11168	17728	20511	10065
% completeness ^a	99.5 (99.6)	96.4 (96.3)	94.6 (95.1)	91.9 (91.4)
$R_{\text{merge}}^{\text{a,b}}$	0.045 (0.299)	0.074 (0.308)	0.047 (0.343)	0.081 (0.336)
Refinement Statistics				
resolution range (Å) ^a	38.04–2.40 (2.49–2.40)	26.98–2.00 (2.11–2.00)	29.74–1.90 (2.00–1.90)	33.01–2.40 (2.53–2.40)
R factor ($R_{\text{free}}/R_{\text{work}}$) ^{a,c}	0.273/0.225	0.279/0.219	0.248/0.209	0.256/0.218

^aValues in parentheses are for the highest-resolution shell. ^b $R_{\text{merge}} = \sum |I_{hkl} - \langle I_{hkl} \rangle| / (\sum I_{hkl})$, where $\langle I_{hkl} \rangle$ is the mean intensity of all reflections equivalent to reflection hkl . ^c $R_{\text{work}} (R_{\text{free}}) = \sum \|F_{\text{obs}}\| - \|F_{\text{calc}}\| / \sum \|F_{\text{obs}}\|$, where 5% of randomly selected data were used for R_{free} .

than natural hormone **1a**. All three analogues **5a–c** showed potent transcriptional activity (Figure 1). 22-Ethyl analogue **5b** acts as a full agonist, whereas **3b** and **4b** are partial agonists. More surprisingly, 22-butyl analogue **5c** completely restored agonistic activity, although **2** and **3c** are antagonists and **4c** is a quite weak agonist.

This drastic change in transcriptional activity was explained by comparison of the crystal structures. As expected, **5c** induced the formation of a butyl pocket similar to **2** (Figure

3b), but in contrast to **2**, **5c** interacts intimately with helix 12 to form a stable complex with VDR. As shown in Table 3, the number of amino acid residues within 4.5 Å of **5c** is 27, whereas for **2** there are only 22 residues within that distance. Compound **5c** therefore forms sufficient interactions with VDR, and especially with helix 12, to form a stable complex, but **2** does not. This is a primary reason why **2** is an antagonist whereas **5c** is an agonist.

Table 3. Residues within 4.5 Å from ligand

compd	residues within 4.5 Å from ligand
1a (28 residues) ^a	Tyr143, Tyr147, Phe150, Leu223, Leu226, Leu229, Val230, Ser233, Ile264, Ile267, Met268, Arg270, Ser271, Ser274, Trp282, Cys284, Tyr291, Val296, Ala299, His301, Leu305, Leu309, His393, Tyr397, Leu400, Leu410, Val414, Phe418
2 (22 residues) ^a	Tyr143, Tyr147, Phe150, Leu226, Leu229, Val230, Ser233, Ile264, Ile267, Met268, Arg270, Ser271, Ser274, Trp282, Cys284, Tyr291, Val296, His301, Leu305, Leu309, His393, Leu398
3a (20 residues) ^a	Tyr143, Tyr147, Phe150, Leu226, Leu229, Val230, Ser233, Ile264, Ile267, Met268, Arg270, Ser271, Ser274, Trp282, Cys284, Tyr291, Val296, His301, Leu309, His393
4a (24 residues) ^a	Tyr143, Tyr147, Phe150, Leu223, Leu226, Leu229, Val230, Ser233, Ile264, Ile267, Met268, Arg270, Ser271, Ser274, Trp282, Cys284, Tyr291, Val296, Ala299, His301, Leu305, His393, Tyr397, Phe418
5a (27 residues) ^a	Tyr143, Tyr147, Phe150, Leu223, Leu226, Ala227, Leu229, Val230, Ser233, Ile264, Ile267, Met268, Arg270, Ser271, Ser274, Trp282, Cys284, Tyr291, Val296, Ala299, His301, Leu305, Leu309, His393, Tyr397, Val414, Phe418
5c (27 residues) ^a	Tyr143, Tyr147, Phe150, Leu223, Leu226, Leu229, Val230, Ser233, Ile264, Ile267, Met268, Arg270, Ser271, Ser274, Trp282, Cys284, Tyr291, Val296, Ala299, His301, Leu305, Leu309, His393, Tyr397, Leu410, Val414, Phe418

^aTotal number of residues within 4.5 Å from ligand.

Interestingly, the butyl pocket of the VDR-LBD/5c complex is slightly smaller than that of VDR-LBD/2; this is mainly due to the conformation of Met268 and Leu305 (Figure 3c). The terminal S-methyl group of Met268 in the VDR-LBD/2 complex rotated in about 120° compared with that in the VDR-LBD/1a complex, but that in VDR-LBD/5c did not rotate. In addition, Leu305 adopted a conformation intermediate between conformations of the complexes with 1a and 2. Furthermore, we found that 5c and Phe418 in helix 12 make C–H... π interactions (Figure 3d). The distance between the terminal carbon of one of the 24-ethyl groups in 5c and the center of the π -system ($d_{C-\pi}$) is 3.9 Å, indicating that this C–H... π interaction would contribute significantly to the overall stability of the protein.³² The results agree well with our hypothesis that increased hydrophobic interactions overcome the strain caused by the formation of an extra cavity such as a butyl pocket.

In 22-H analogues, the EC₅₀ of transcriptional activity decreased in the order 3a > 4a > 5a. These results are explained by the crystal structures. Specific differences between the three complexes are observed in the interactions between the ligand side chain and the C-terminus of VDR-LBD. As shown in Figure 2b, among the C-terminal residues within 4.5 Å of hormone 1a, five residues (Tyr397, Leu400, Leu410, Val414, and Phe418), three residues (Leu400, Leu410, and Val414), and two residues (Leu400 and Leu410) are not within 4.5 Å of 3a, 4a, and 5a, respectively, indicating that interactions with helices 11 and 12 increase in the order 3a < 4a < 5a. These results indicate that intimate interactions with VDR reinforce transcriptional activity.

Structural modification of the secondary structure of a protein by the binding of a small molecule such as a ligand, a substrate, or an inhibitor is difficult, but modification of a loop region would be possible. Our synthetic compounds with a 22-butyl substituent, 2 and 5c, push out the loop region, as observed in the crystal structures. This study suggests that modification of the three-dimensional structure of a protein at a flexible loop region by a ligand binding is a novel strategy for the discovery of new drugs that have the desired selectivity.

CONCLUSIONS

We designed and synthesized analogues 5a–c bearing a diethyl substituent at C(24) and evaluated their biological activities. The crystal structures of VDR-LBD complexed with 3a, 4a, 5a, or 5c were solved and the results confirmed the following. First, analogues with a 22S-butyl group, such as 2 and 5c, induce butyl pocket formation to accommodate the butyl group.

Second, among ligands that induce butyl pocket formation (2, 3c, and 5c), a ligand acts as an antagonist when it does not interact with the C-terminus of VDR, whereas a ligand acts as an agonist when it interacts intimately with the C-terminus of VDR. Third, ligands that do not induce an extra cavity like a butyl pocket (3a, 4a, and 5a) increase agonistic activity when the ligand increases interactions with the C-terminus of VDR. Thus, butyl pocket formation in VDR strongly affects the agonistic or antagonistic behavior of ligands. These results indicate that structural modification of a target protein at a flexible region such as loop region may be an important strategy for the discovery of new drugs for the treatment of various diseases.

EXPERIMENTAL SECTION

All reagents were purchased from commercial sources. Unless otherwise stated, NMR spectra were recorded at 300 MHz for ¹H NMR and 75 MHz for ¹³C NMR in CDCl₃ solution with TMS as an internal standard, and the chemical shifts are given in δ values. High and low resolution mass spectra were obtained with JEOL JMS D-300, JEOL AccuTOF LC-plus JMS-T100LP, and JEOL JMS-HX110A spectrometers. Relative intensities are given in parentheses in low mass. IR spectra were recorded on a Shimadzu FTIR-8400S spectrophotometer, and data are given in cm⁻¹. UV spectra were recorded on a Beckman DU7500 spectrophotometer. All air and moisture sensitive reactions were carried out under argon or nitrogen atmosphere. Purity was determined by HPLC [PEGASIL silica SP100, 4.6 mm \times 150 mm, hexane/CHCl₃/MeOH (100:25:8), flow rate 1.0 mL/min] and was >95% for all compounds tested.

6-[(1R,3R,7E,17 β)-1,3-Bis[[tert-butyl(dimethyl)silyloxy]-2-methylidene-9,10-secoestra-5,7-dien-17-yl]-3-ethylheptan-3-ol (7). To a solution of ester 6 (54.6 mg, 0.0867 mmol) in THF (1 mL) at -78 °C was added EtLi (870 μ L of 0.5 M benzene/cyclohexane (90/10) solution, 0.435 mmol), and the mixture was stirred for 1 h. The reaction was quenched with saturated NH₄Cl, and the mixture was extracted with AcOEt. The organic layer was washed with brine, dried over MgSO₄, and evaporated. The residue was chromatographed on silica gel (AcOEt/hexane = 5/95) to afford 7 (30.4 mg, 0.0462 mmol, 53%). ¹H NMR δ 0.02, 0.05, 0.06, 0.08 (each 3 H, s, SiMe), 0.55 (3 H, s, H-18), 0.80–0.96 (6H, m, CH₂CH₃ \times 2), 0.86, 0.89 (each 9 H, s, t-Bu), 0.94 (3 H, d, J = 6.1 Hz, H-21), 2.80 (1 H, m, H-9), 4.42 (2 H, m, H-1, 3), 4.92, 4.96 (each 1 H, s, -C=CH₂), 5.83 (1 H, d, J = 11.1 Hz, H-7), 6.21 (1 H, d, J = 11.1 Hz, H-6). ¹³C NMR δ -5.1, -4.9, -4.8 (2 C), 7.7, 7.9, 12.0, 18.1, 18.2, 18.9, 22.2, 23.4, 25.7 (3 C), 25.8 (3 C), 27.7, 28.7, 29.2, 30.9, 31.1, 34.2, 36.5, 38.6, 40.6, 45.6, 47.6, 56.2, 56.3, 71.7, 72.5, 74.7, 106.2, 116.1, 122.4, 132.7, 141.1, 152.9. MS (EI) *m/z* (%): 658 (M⁺, 2), 526 (26), 508 (8), 366 (20), 234 (14), 147 (15), 73 (100). HRMS (EI) calcd for C₄₀H₇₄O₃Si₂ 658.5177, found 658.5196. IR (neat) 2954, 2856, 1461, 1251, 1101, 1072, 835 cm⁻¹. UV (hexane) λ_{max} 246, 254, 264 nm.

2-Methylidene-26,27-dimethyl-19,24-dinor-1 α ,25-dihydroxyvitamin D₃ (5a). A solution of **7** (29.4 mg, 0.0447 mmol) and camphor sulfonic acid (39.0 mg, 0.168 mmol) in MeOH (1 mL) was stirred at room temperature for 0.5 h. Aqueous NaHCO₃ was added, and the mixture was extracted with AcOEt. The organic layer was washed with brine, dried over MgSO₄, and evaporated. The residue was chromatographed on silica gel (AcOEt/hexane = 1/1) to afford **5a** (17.0 mg, 89%). ¹H NMR δ 0.55 (3 H, s, H-18), 0.86 (6H, td, J = 2.0, 7.4 Hz, CH₂CH₃ \times 2), 0.95 (3 H, d, J = 6.0 Hz, H-21), 4.47 (2 H, m, H-1, 3), 5.09, 5.11 (each 1 H, s, -C=CH₂), 5.88 (1 H, d, J = 11.2 Hz, H-7), 6.36 (1 H, d, J = 11.2 Hz, H-6). ¹³C NMR δ 7.7, 7.8, 12.1, 18.9, 22.3, 23.5, 27.6, 29.0, 29.1, 30.9, 31.1, 34.2, 36.4, 38.1, 40.4, 45.8 (2 C), 56.2, 56.3, 70.6, 71.8, 74.7, 107.7, 115.3, 124.2, 130.5, 143.4, 152.0. MS (EI) m/z (%): 430 (M⁺, 40), 383 (36), 365 (25), 285 (32), 187 (20), 175 (30), 161 (46), 147 (57), 135 (75), 119 (55), 69 (100). HRMS (EI) calcd for C₂₈H₄₆O₃ 430.3447, found 430.3462. IR (neat) 3377, 2941, 2875, 1658, 1612, 1452, 1145, 1074, 1045, 977, 912, 756 cm⁻¹. UV (EtOH) λ_{\max} 245, 254, 263 nm.

(5S,6R)-6-[1-[(1R,3R,7E,17 β)-1,3-Bis[[tert-butyl(dimethyl)silyloxy]-2-methylidene-9,10-secoestra-5,7-dien-17-yl]ethyl]-3,5-diethylheptan-3-ol (9). To a solution of ester **8** (118.9 mg, 0.18 mmol) in THF (3 mL) at room temperature was added EtMgBr (530 μ L of 1.0 M THF solution, 0.53 mmol), and the mixture was stirred for 3 h. The reaction was quenched with saturated NH₄Cl, and the mixture was extracted with AcOEt. The organic layer was washed with brine, dried over MgSO₄, and evaporated. The residue was chromatographed on silica gel (AcOEt/hexane = 3/97) to afford **9** (104.0 mg, 0.15 mmol) in 86% yield. ¹H NMR δ 0.03, 0.04, 0.06, 0.08 (each 3 H, s, SiMe), 0.53 (3 H, s, H-18), 0.83 (3 H, J = 6.3 Hz, d, H-21), 0.84–0.94 (9H, m, CH₂CH₃ \times 3), 0.86, 0.89 (each 9 H, s, *t*-Bu), 2.82 (1 H, m, H-9), 4.42 (2 H, m, H-1,3), 4.92, 4.96 (each 1 H, s, -C=CH₂), 5.84 (1 H, d, J = 11.1 Hz, H-7), 6.21 (1 H, d, J = 11.1 Hz, H-6). ¹³C NMR δ -4.8, -4.69, -4.66, -4.63, 8.2, 8.3, 12.2, 13.5, 13.8, 18.4, 18.5, 22.3, 22.4, 23.7, 26.0 (3 C), 26.1 (3 C), 27.7, 29.0, 31.0, 32.0, 37.4, 38.9, 39.9, 40.3, 40.9, 45.9, 47.8, 54.8, 56.5, 71.9, 72.6, 75.8, 106.5, 116.3, 122.6, 133.0, 141.5, 153.2. MS (APCI) m/z (%): 711 (M + Na⁺, 1), 429 (45), 234 (35), 220 (25), 202 (100), 167 (95). HRMS (APCI) calcd for C₄₂H₇₉O₃Si₂Na 710.5465, found 710.5462. IR (neat) 3489, 2955, 2930, 2883, 2856, 1730, 1655, 1618, 1472, 1462, 1256, 1101, 935, 897, 835, 775, 667 cm⁻¹. UV (hexane) λ_{\max} 246, 255, 265 nm.

225-Ethyl-2-methylidene-26,27-dimethyl-19,24-dinor-1 α ,25-dihydroxyvitamin D₃ (5b). In a manner similar to that for the synthesis of **5a** from **7**, target compound **5b** (55.0 mg, 0.120 mmol) was obtained from **9** (83.8 mg, 0.122 mmol) in 98% yield. ¹H NMR δ 0.53 (3 H, s, H-18), 0.81 (3 H, J = 6.3 Hz, d, H-21), 0.81–0.93 (9H, m, CH₂CH₃ \times 3), 2.81 (1 H, m, H-9), 4.44 (2 H, m, H-1,3), 5.06, 5.08 (each 1 H, s, -C=CH₂), 5.87 (1 H, d, J = 11.1 Hz, H-7), 6.33 (1 H, d, J = 11.1 Hz, H-6). ¹³C NMR δ 7.9, 8.0, 12.1, 13.3, 13.6, 22.2 (2 C), 23.6, 27.4, 29.0, 30.8, 31.7, 37.2, 38.1, 39.5, 40.0, 40.6, 45.8 (2 C), 54.6, 56.3, 70.6, 71.8, 75.7, 107.7, 115.3, 124.1, 130.6, 143.3, 152.0. MS (APCI) m/z (%): 481 (M + Na⁺, 100), 437 (52), 429 (23). HRMS (APCI) calcd for C₃₀H₅₀O₃Na 481.3658 found 481.3664. IR (neat) 3390, 2961, 2939, 2874, 1715, 1651, 1614, 1462, 1456, 1381, 1074, 1045, 978, 912, 756, 667 cm⁻¹. UV (EtOH) λ_{\max} 246, 254, 264 nm.

(5S)-4-[1-[(1R,3R,7E,17 β)-1,3-Bis[[tert-butyl(dimethyl)silyloxy]-2-methylidene-9,10-secoestra-5,7-dien-17-yl]ethyl]-3-ethylnonan-3-ol (11). To a solution of EtMgI in Et₂O (2 mL) prepared from EtI (91 μ L, 1.13 mmol) and magnesium turnings (27.3 mg, 1.13 mmol) was added ester **10** (37.8 mg, 0.054 mmol) in Et₂O (1 mL) at room temperature, and the mixture was stirred for 3.5 h. The reaction was quenched with 1 N HCl, and the mixture was extracted with AcOEt. The organic layer was washed with saturated NaHCO₃ and brine, dried over MgSO₄, and evaporated. The residue was chromatographed on silica gel (AcOEt/hexane = 5/95) to afford **11** (26.7 mg, 0.0374 mmol) in 69% yield. ¹H NMR δ 0.03, 0.04, 0.06, 0.08 (each 3 H, s, SiMe), 0.53 (3 H, s, H-18), 0.83 (3 H, d, J = 6.6 Hz, H-21), 0.80–0.94 (9H, m, CH₂CH₃ \times 3), 0.86, 0.89 (each 9 H, s, *t*-Bu), 2.82 (1 H, m, H-9), 4.42 (2 H, m, H-1, 3), 4.92, 4.97 (each 1 H, s,

-C=CH₂), 5.83 (1 H, d, J = 11.1 Hz, H-7), 6.21 (1 H, d, J = 11.1 Hz, H-6); ¹³C NMR δ -5.1, -4.9, -4.8 (2 C), 7.9, 8.1, 12.0, 13.5, 14.2, 18.1, 18.2, 22.1, 23.3, 23.5, 25.7 (3 C), 25.8 (3 C), 27.5, 28.8, 29.4, 30.7, 30.9, 31.7, 35.1, 38.6, 39.5, 40.6, 40.7, 45.6, 47.5, 54.5, 56.2, 71.7, 72.4, 75.6, 106.2, 116.1, 122.4, 132.7, 141.2, 152.9. MS (EI) m/z (%): 714 (M⁺, 2), 582 (36), 564 (10), 366 (35), 351 (10), 257 (11), 234 (12), 197 (10), 147 (15), 73 (100). HRMS (EI) calcd for C₄₄H₈₂O₃Si₂ 714.5802, found 714.5804. IR (neat) 3487, 2954, 2927, 2856, 1726, 1658, 1620, 1461, 1251, 1101, 1072, 835, 775 cm⁻¹. UV (hexane) λ_{\max} 246, 255, 264 nm.

225-Butyl-2-methylidene-26,27-dimethyl-19,24-dinor-1 α ,25-dihydroxyvitamin D₃ (5c). In a manner similar to that for the synthesis of **5a** from **7**, target compound **5c** (16.6 mg, 0.0342 mmol) was obtained from **11** (26.7 mg, 0.0374 mmol) in 91% yield. ¹H NMR δ 0.54 (3 H, s, H-18), 0.82 (3 H, d, J = 6.3 Hz, H-21), 0.86 (6 H, t, J = 7.4 Hz, 2 \times CH₃ of Et), 0.90 (3 H, t, J = 6.8 Hz, CH₃ of Bu), 4.47 (2 H, m, H-1, 3), 5.09, 5.11 (each 1 H, s, -C=CH₂), 5.88 (1 H, d, J = 11.2 Hz, H-7), 6.35 (1 H, d, J = 11.2 Hz, H-6). ¹³C NMR δ 7.9, 8.0, 12.1, 13.5, 14.2, 22.1, 23.3, 23.5, 27.4, 29.0, 29.4, 30.8 (2 C), 31.6, 35.1, 38.1, 39.3, 40.5 (2 C), 45.8 (2 C), 54.5, 56.3, 70.6, 71.8, 75.6, 107.7, 115.2, 124.2, 130.4, 143.4, 152.0. MS (EI) m/z (%): 486 (M⁺, 31), 439 (15), 421 (10), 384 (22), 315 (18), 285 (20), 269 (10), 251 (12), 231 (10), 173 (20), 153 (60), 135 (95), 119 (40), 105 (70), 91 (70), 81 (75), 69 (100). HRMS (EI) calcd for C₃₂H₅₄O₃ 486.4072, found 486.4073. IR (neat) 3388, 2933, 2871, 1712, 1658, 1612, 1456, 1380, 1076, 910, 754 cm⁻¹. UV (EtOH) λ_{\max} 246, 254, 263 nm.

Competitive Binding Assay, Human VDR. The human recombinant VDR ligand-binding domain (LBD) was expressed as an N-terminal GST-tagged protein in *E. coli* BL21 (DE3) pLys S (Promega).³¹ The cells were lysed by sonication. The supernatants were diluted approximately 500 times in 50 mM Tris buffer (100 mM KCl, 5 mM DTT, 0.5% CHAPS, pH 7.5) containing bovine serum albumin (100 μ g/mL). Binding to GST-hVDR-LBD was evaluated according to the procedure reported.³³ The receptor solution (570 μ L) in an assay tube was incubated with [³H]-1 α ,25-dihydroxyvitamin D₃ (specific activity, 5.85 TBq/mmol, ~2000 cpm) together with graded amounts of each vitamin D analogue (0.001–100 nM) or vehicle for 16 h at 4 °C. The bound and free [³H]-1 α ,25-dihydroxyvitamin D₃ molecules were separated by treating with dextran-coated charcoal for 30 min at 4 °C. The assay tubes were centrifuged at 1000g for 10 min. The radioactivity of the supernatant was counted. Nonspecific binding was subtracted. These experiments were done in duplicate.

Transfection and Transactivation Assay. COS-7 cells were cultured in Dulbecco's modified Eagle's medium (DMEM) supplemented with 5% fetal bovine serum (FBS). Cells were seeded on 24-well plates at a density of 2 \times 10⁴ per well. After 24 h, the cells were transfected with a reporter plasmid containing three copies of the mouse osteopontin VDRE (5'-GGTTCAcgaGGTTCA, SPPx3-TK-Luc), a wild-type or mutant hVDR expression plasmid (pCMX-hVDR), and the internal control plasmid containing sea pansy luciferase expression constructs (pRL-CMV) by the lipofection method as described previously.¹² After an 8 h incubation, the cells were treated with either the ligand or ethanol vehicle and cultured for 16 h. Cells in each well were harvested with a cell lysis buffer, and the luciferase activity was measured with a luciferase assay kit (Promega, WI, U.S.). Transactivation measured by the luciferase activity was normalized with the internal control. All experiments were done in triplicate.

Protein Expression. The rat VDR-LBD (residues 116–423, Δ 165–211) was subcloned as an N-terminal His₆-tagged fusion protein into the pET-28a vector. *E. coli* Rosetta 2 (DE3) was freshly transformed with the plasmid and grown in four flasks containing 0.75 L of 2xTY medium with kanamycin, 34 μ g/mL, and chloramphenicol, 50 μ g/mL, at 37 °C until an OD of 0.8 was obtained. The cultures were then induced with 0.5 mM isopropyl- β -D-thiogalactopyranoside and further incubated at 23 °C for 18 h. Cells were harvested and resuspended in 50 mL of lysis buffer (50 mM Na/K phosphate, pH 8.0, 10 mM imidazole, 500 mM NaCl, 5% glycerol, 1% Tween 20, 1 mM TCEP, 1 mM PMSF). Cells were lysed by sonication, and the

soluble fraction was isolated by centrifugation (18000g for 20 min). The supernatant was applied to Ni-NTA agarose (Qiagen, Santa Clarita, CA), and the resin was thoroughly washed in wash buffer (50 mM Na/K phosphate, pH 8.0, 20 mM imidazole, 500 mM NaCl, 5% glycerol, 1% Tween 20, 1 mM TCEP, 1 mM PMSF). The rat VDR-LBD was eluted with elution buffer (150 mM imidazole, 50 mM Na/K phosphate, pH 8.0, 500 mM NaCl, 5% glycerol, 1% Tween 20, 1 mM TCEP, 1 mM PMSF). The protein was dialyzed overnight against dialysis buffer A (20 mM Na/K phosphate, pH 7.0, 5% glycerol, 1 mM EDTA, 0.5 mM DTT) and then loaded onto a HiTrap SP HP (1 mL) column (GE Healthcare) equilibrated with buffer A. The elution was performed by NaCl gradient buffer from 0 to 1.0 M. His-tag of the protein in elution mixture (17 mL) was cleaved by addition of 70 units of thrombin and subsequent incubation at 23 °C for 18 h. Then NaCl (1.96 g) was added to the digested mixture (17 mL), and the resulting mixture was passed through a HiTrap benzamidine FF (1 mL) column (GE healthcare). The flow-through was further purified by Superdex S75 gel filtration (25 mL) column (GE Healthcare) with a buffer (100 mM NaCl, Tris-HCl, pH 7.0). Purified rat VDR-LBD was concentrated in buffer B (10 mM Tris-HCl, pH 7.0, 2 mM Na₂N₃, 10 mM DTT, 0.5 mM PMSF) to 7.5 mg/mL, which was estimated by UV absorbance at 280 nm.

X-ray Crystallographic Analysis. A ligand (~10 equiv) was added to the rVDR-LBD, and then coactivator peptide (H₂N-KNHPMLMNLKDN-CONH₂) derived from DRIP205 in buffer C (25 mM Tris-HCl, pH 8.0; 50 mM NaCl; 10 mM DTT; 2 mM Na₂N₃) was added. The mixture of VDR-LBD/ligand/peptide was allowed to crystallize by the vapor diffusion method using a series of precipitant solutions containing 0.1 M MOPS-Na (pH 7.0) or 0.1 M MES-Na (pH 7.0), 0.05–0.4 M sodium formate, 12–22% (w/v) PEG4000, and 5% ethylene glycol. Droplets for crystallization were prepared by mixing 1 μL of complex solution and 1 μL of precipitant solution, and droplets were equilibrated against 300 μL of precipitant solution at 20 °C. Prior to diffraction data collection, crystals were soaked in a cryoprotectant solution containing 0.1 M MOPS-Na, pH 7.0, or 0.1 M MES-Na, pH 7.0, 0.05–0.3 M sodium formate, 12–22% (w/v) PEG4000, and 5% ethylene glycol. Diffraction data sets were collected at 100 K in a stream of nitrogen gas at beamline BL-6A of KEK-PF or NW-12A of KEK-PFAR (Tsukuba, Japan). Reflections were recorded with an oscillation range per image of 1.0°. Diffractions data were indexed, integrated, and scaled using the program iMOSFLM^{34,35}. The structures of ternary complex were solved by molecular replacement with the software Phaser³⁶ in the CCP4 program³⁷ using a rat VDR-LBD coordinates (PDB code 2ZLC), and finalized sets of atomic coordinates were obtained after iterative rounds of model modification with the program Coot³⁸ and refinement with refmac5.^{39–43} The coordinate data for the structures were deposited in Protein Data Bank with accession numbers 3VRT (VDR-LBD/3a complex), 3VRU (VDR-LBD/4a complex), 3VRV (VDR-LBD/5a complex), and 3VRW (VDR-LBD/5c complex).

Graphical Manipulations and Ligand Docking. Graphical manipulations were performed using SYBYL 8.0 (Tripos, St. Louis). The atomic coordinates of the crystal structure of rVDR-LBD complexed with 1a were retrieved from Protein Data Bank (PDB) (entry 2ZLC).²⁴

AUTHOR INFORMATION

Corresponding Author

*Phone: +81 42 721 1580. Fax: +81 42 721 1580. E-mail: yamamoto@ac.shoyaku.ac.jp.

Author Contributions

[†]These authors contributed equally.

Notes

The authors declare no competing financial interest.

ACKNOWLEDGMENTS

Part of this work was supported by a Grant-in-Aid for Scientific Research (Grant 23590135) and a Grant-in-Aid for High

Technology Research Center Project (Grant 19-8) from the Ministry of Education, Culture, Sports, Science and Technology, Japan. The synchrotron-radiation experiment was performed at the Photon Factory (Proposal Grants 2008G169 and 2009G647). We acknowledge the help provided by the beamline scientists at the Photon Factory.

ABBREVIATIONS USED

VDR, vitamin D receptor; LBP, ligand binding pocket; RXR, retinoid X receptor; LBD, ligand binding domain

REFERENCES

- (1) Feldman, D., Pike, J. W., Glorieux, F. H., Eds. *Vitamin D*, 2nd ed.; Elsevier Academic Press: Amsterdam, 2005.
- (2) Jurutka, P. W.; Whitfield, G. K.; Hsieh, J. C.; Thompson, P. D.; Haussler, C. A.; Haussler, M. R. Molecular nature of the vitamin D receptor and its role in regulation of gene expression. *Rev. Endocr. Metab. Disord.* **2001**, *2*, 203–216.
- (3) Yamada, S.; Shimizu, M.; Yamamoto, K. Vitamin D Receptor. In *Vitamin D and Rickets*; Hochberg, Z., Ed.; Endocrine Development, Vol. 6; Karger: Basel, Switzerland, 2003; pp 50–68.
- (4) Binderup, L.; Binderup, E.; Godtfredsen, W. O. Development of New Vitamin D Analogs. In *Vitamin D*, 2nd ed.; Feldman, D., Pike, J. W., Glorieux, F. H., Eds.; Elsevier Academic Press: Amsterdam, 2005; pp 1027–1043.
- (5) Kubodera, N. Pharmaceutical studies on vitamin D derivatives and practical syntheses of six commercially available vitamin D derivatives that contribute to current clinical practice. *Heterocycles* **2010**, *80*, 83–98.
- (6) Bury, Y.; Steinmeyer, A.; Carlberg, C. Structure activity relationship of carboxylic ester antagonists of the vitamin D₃ receptor. *Mol. Pharmacol.* **2000**, *58*, 1067–1074.
- (7) Igarashi, M.; Yoshimoto, N.; Yamamoto, K.; Shimizu, M.; Makishima, M.; DeLuca, H. F.; Yamada, S. Identification of a highly potent vitamin D receptor antagonist: (25S)-26-adamantyl-25-hydroxy-2-methylene-22,23-didehydro-19,27-dinor-20-epi-vitamin D₃ (ADMI3). *Arch. Biochem. Biophys.* **2007**, *460*, 240–253.
- (8) Miura, D.; Manabe, K.; Ozono, K.; Saito, M.; Gao, Q.; Norman, A. W.; Ishizuka, S. Antagonistic activity of novel 1 α ,25-dihydroxyvitamin D₃-26,23-lactone analogs on differentiation of human leukemia cells (HL-60) induced by 1 α ,25-dihydroxyvitamin D₃. *J. Biol. Chem.* **1999**, *274*, 16392–16399.
- (9) (a) Ishizuka, S.; Kurihara, N.; Miura, D.; Takenouchi, K.; Cornish, J.; Cundy, T.; Reddy, S. V.; Roodman, G. D. Vitamin D antagonist, TEI-9647, inhibits osteoclast formation induced by 1 α ,25-dihydroxyvitamin D₃ from pagetic bone marrow cells. *J. Steroid Biochem. Mol. Biol.* **2004**, *89–90*, 331–334. (b) Roodman, G. D.; Windle, J. J. Paget disease of bone. *J. Clin. Invest.* **2005**, *115*, 200–208.
- (10) Saito, N.; Saito, H.; Anzai, M.; Yoshida, A.; Fujishima, T.; Takenouchi, K.; Miura, D.; Ishizuka, S.; Takayama, H.; Kittaka, A. Dramatic enhancement of antagonistic activity on vitamin D receptor: a double functionalization of 1 α -hydroxyvitamin D₃ 26,23-lactones. *Org. Lett.* **2003**, *5*, 4859–4862.
- (11) Yoshimoto, N.; Inaba, Y.; Yamada, S.; Makishima, M.; Shimizu, M.; Yamamoto, K. 2-Methylene 19-nor-25-dehydro-1 α -hydroxyvitamin D₃ 26,23-lactones: synthesis, biological activities and molecular basis of passive antagonism. *Bioorg. Med. Chem.* **2008**, *16*, 457–473.
- (12) Inaba, Y.; Yoshimoto, N.; Sakamaki, Y.; Nakabayashi, M.; Ikura, T.; Tamamura, H.; Ito, N.; Shimizu, M.; Yamamoto, K. A new class of vitamin D analogues that induce structural rearrangement of the ligand-binding pocket of the receptor. *J. Med. Chem.* **2009**, *52*, 1438–1449.
- (13) Rochel, N.; Wurtz, J. M.; Mitschler, A.; Klaholz, B.; Moras, D. The crystal structure of the nuclear receptor for vitamin D bound to its natural ligand. *Mol. Cell* **2000**, *5*, 173–179.
- (14) Tocchini-Valentini, G.; Rochel, N.; Wurtz, J. M.; Mitschler, A.; Moras, D. Crystal structures of the vitamin D receptor complexed to

super agonist 20-epi ligands. *Proc. Natl. Acad. Sci. U.S.A.* **2001**, *98*, 5491–5496.

(15) Vanhooke, J. L.; Benning, M. M.; Bauer, C. B.; Pike, J. W.; DeLuca, H. F. Molecular structure of the rat vitamin D receptor ligand binding domain complexed with 2-carbon-substituted vitamin D₃ hormone analogues and a LXXLL-containing coactivator peptide. *Biochemistry* **2004**, *43*, 4101–4110.

(16) Ciesielski, F.; Rochel, N.; Mitschler, A.; Kouzmenko, A.; Moras, D. Structural investigation of the ligand binding domain of the zebrafish VDR in complexes with 1 α ,25(OH)₂D₃ and Gemini: purification, crystallization and preliminary X-ray diffraction analysis. *J. Steroid Biochem. Mol. Biol.* **2004**, *89–90*, 55–59.

(17) Tocchini-Valentini, G.; Rochel, N.; Wurtz, J. -M.; Moras, D. Crystal structures of the vitamin D nuclear receptor liganded with the vitamin D side chain analogues calcipotriol and seocalcitol, receptor agonists of clinical importance. Insights into a structural basis for the switching of calcipotriol to a receptor antagonist by further side chain modification. *J. Med. Chem.* **2004**, *47*, 1956–1961.

(18) Eelen, G.; Verlinden, L.; Rochel, N.; Claessens, F.; De Clercq, P.; Vandewalle, M.; Tocchini-Valentini, G.; Moras, D.; Bouillon, R.; Verstuyf, A. Superagonistic action of 14-epi-analogs of 1,25-dihydroxyvitamin D explained by vitamin D receptor–coactivator interaction. *Mol. Pharmacol.* **2005**, *67*, 1566–1573.

(19) Hourai, S.; Fujishima, T.; Kittaka, A.; Suhara, Y.; Takayama, H.; Rochel, N.; Moras, D. Probing a water channel near the A-ring of receptor-bound 1 α ,25-dihydroxyvitamin D₃ with selected 2 α -substituted analogues. *J. Med. Chem.* **2006**, *49*, 5199–5205.

(20) Ciesielski, F.; Rochel, N.; Moras, D. Adaptability of the vitamin D nuclear receptor to the synthetic ligand Gemini: remodelling the LBP with one side chain rotation. *J. Steroid Biochem. Mol. Biol.* **2007**, *103*, 235–242.

(21) Rochel, N.; Hourai, S.; Perez-Garcia, X.; Rumbo, A.; Mourino, A.; Moras, D. Crystal structure of the vitamin D nuclear receptor ligand binding domain in complex with a locked side chain analog of calcitriol. *Arch. Biochem. Biophys.* **2007**, *460*, 172–176.

(22) Vanhooke, J. L.; Tadi, B. P.; Benning, M. M.; Plum, L. A.; DeLuca, H. F. New analogs of 2-methylene-19-nor-(20S)-1,25-dihydroxyvitamin D₃ with conformationally restricted side chains: evaluation of biological activity and structural determination of VDR-bound conformations. *Arch. Biochem. Biophys.* **2007**, *460*, 161–165.

(23) Hourai, S.; Rodrigues, L. C.; Antony, P.; Reina-San-Martin, B.; Ciesielski, F.; Magnier, B. C.; Schoonjans, K.; Mourino, A.; Rochel, N.; Moras, D. Structure-based design of a superagonist ligand for the vitamin D nuclear receptor. *Chem. Biol.* **2008**, *15*, 383–392.

(24) Shimizu, M.; Miyamoto, Y.; Takaku, H.; Matsuo, M.; Nakabayashi, M.; Masuno, H.; Udagawa, N.; DeLuca, H. F.; Ikura, T.; Ito, N. 2-Substituted-16-ene-22-thia-1 α ,25-dihydroxy-26,27-dimethyl-19-nor-vitamin D₃ analogs: synthesis, biological evaluation, and crystal structure. *Bioorg. Med. Chem.* **2008**, *16*, 6949–6964.

(25) Nakabayashi, M.; Yamada, S.; Yoshimoto, N.; Tanaka, T.; Igarashi, M.; Ikura, T.; Ito, N.; Makishima, M.; Tokiwa, H.; Deluca, H. F.; Shimizu, M. Crystal structures of rat vitamin D receptor bound to adamantyl vitamin D analogs: structural basis for vitamin D receptor antagonism and partial agonism. *J. Med. Chem.* **2008**, *51*, 5320–5329.

(26) Uskokovic, M. R.; Manchand, P. S.; Peleg, S.; Norman, A. W. Synthesis and Preliminary Evaluation of the Biological Properties of a 1 α ,25-Dihydroxyvitamin D₃ Analogue with Two Side-Chains. In *Vitamin D: Chemistry, Biology and Clinical Applications of the Steroid Hormone*; Norman, A. W., Bouillon, R., Thomasset, M., Eds.; University of California: Riverside, CA, 1997; pp19–21.

(27) Kurek-Tyrlík, A.; Makaev, F. Z.; Wicha, J.; Zhabinskii, V.; Calverley, M. J. Pivoting 20-Normal and 20-Epi Calcitriols: Synthesis and Crystal Structure of a “Double Side Chain” Analogue. In *Vitamin D: Chemistry, Biology and Clinical Applications of the Steroid Hormone*; Norman, A. W., Bouillon, R., Thomasset, M., Eds.; University of California: Riverside, CA, 1997; pp 30–31.

(28) Sakamaki, Y.; Inaba, Y.; Yoshimoto, N.; Yamamoto, K. Potent antagonist for the vitamin D receptor: vitamin D analogues with simple side chain structure. *J. Med. Chem.* **2010**, *53*, 5813–5826.

(29) Sicinski, R. R.; Prahl, J. M.; Smith, C. M.; DeLuca, H. F. New 1 α ,25-dihydroxy-19-norvitamin D₃ compounds of high biological activity: synthesis and biological evaluation of 2-hydroxymethyl, 2-methyl, and 2-methylene analogues. *J. Med. Chem.* **1998**, *41*, 4662–4674.

(30) Yamamoto, K.; Ogura, H.; Jukuta, J.; Inoue, H.; Hamada, K.; Sugiyama, Y.; Yamada, S. Stereochemical and mechanistic studies on conjugate addition of organocuprates to acyclic enones and enoates: simple rule for diastereofacial selectivity. *J. Org. Chem.* **1998**, *63*, 4449–4458.

(31) Inaba, Y.; Yamamoto, K.; Yoshimoto, N.; Matsunawa, M.; Uno, S.; Yamada, S.; Makishima, M. Vitamin D₃ derivatives with adamantane or lactone ring side chains are cell type-selective vitamin D receptor modulators. *Mol. Pharmacol.* **2007**, *71*, 1298–1311.

(32) Brandl, M.; Weiss, M. S.; Jabs, A.; Sühnel, J.; Hilgenfeld, R. C–H $\cdots\pi$ -interactions in proteins. *J. Mol. Biol.* **2001**, *16*, 357–377.

(33) Yamamoto, K.; Sun, W.-Y.; Ohta, M.; Hamada, K.; DeLuca, H. F.; Yamada, S. Conformationally restricted analogs of 1 α ,25-dihydroxyvitamin D₃ and its 20-epimer: compounds for study of the three-dimensional structure of vitamin D responsible for binding to the receptor. *J. Med. Chem.* **1996**, *39*, 2727–2737.

(34) Leslie, A. G. W.; Powell, H. R. In *Evolving Methods for Macromolecular Crystallography*; Read, R. J., Sussman, J. L., Eds.; NATO Science Series II, Vol. 245; Springer Verlag: Dordrecht, The Netherlands, 2007; pp 41–51.

(35) Batty, T. G.; Kontogiannis, L.; Johnson, O.; Powell, H. R.; Leslie, A. G. iMOSFLM: a new graphical interface for diffraction-image processing with MOSFLM. *Acta Crystallogr., Sect. D: Biol. Crystallogr.* **2011**, *67*, 271–281.

(36) McCoy, A. J.; Grosse-Kunstleve, R. W.; Adams, P. D.; Winn, M. D.; Storoni, L. C.; Read, R. J. Phaser crystallographic software. *J. Appl. Crystallogr.* **2007**, *40*, 658–674.

(37) Collaborative Computational Project, Number 4. The CCP4 Suite: Programs for Protein Crystallography. *Acta Crystallogr., Sect. D: Biol. Crystallogr.* **1994**, *50*, 760–763.

(38) Emsley, P.; Lohkamp, B.; Scott, W. G.; Cowtan, K. Features and development of Coot. *Acta Crystallogr., Sect. D: Biol. Crystallogr.* **2010**, *66*, 486–501.

(39) Murshudov, G. N.; Vagin, A. A.; Dodson, E. J. Refinement of macromolecular structures by the maximum-likelihood method. *Acta Crystallogr., Sect. D: Biol. Crystallogr.* **1997**, *53*, 240–255.

(40) Pannu, N. S.; Murshudov, G. N.; Dodson, E. J.; Read, R. J. Incorporation of prior phase information strengthens maximum-likelihood structure refinement. *Acta Crystallogr., Sect. D: Biol. Crystallogr.* **1998**, *54*, 1285–1294.

(41) Winn, M. D.; Isupov, M. N.; Murshudov, G. N. Use of TLS parameters to model anisotropic displacements in macromolecular refinement. *Acta Crystallogr., Sect. D: Biol. Crystallogr.* **2001**, *57*, 122–133.

(42) Steiner, R. A.; Lebedev, A. A.; Murshudov, G. N. Fisher's information in maximum-likelihood macromolecular crystallographic refinement. *Acta Crystallogr., Sect. D: Biol. Crystallogr.* **2003**, *59*, 2114–2124.

(43) Murshudov, G. N.; Skubák, P.; Lebedev, A. A.; Pannu, N. S.; Steiner, R. A.; Nicholls, R. A.; Winn, M. D.; Long, F.; Vagin, A. A. REFMACS for the refinement of macromolecular crystal structures. *Acta Crystallogr., Sect. D: Biol. Crystallogr.* **2011**, *67*, 355–367.